Supplementary Material associated with 'Comparison of time-lapse ground-penetrating radar and electrical resistivity tomography surveys for detecting pig (*Sus* spp.) cadaver graves in an Australian environment'

Table of contents

S1 GPR results pg. 2

S1.1 velocity analysis pg. 2

S2 ERT results pg. 2

S2.1 Mean resistivity value of pig portions of the ERT line pg. 5

S2.2 Mean resistivity value of fill portions of the ERT line pg. 6

S2.3 Mean resistivity value of whole grave portions of the ERT line pg. 6

S2.4 Mean resistivity value of whole non-grave portions of the ERT line pg. 7

S2.5 Comparing the mean resistivity value of whole grave and whole non-grave portions of the ERT line pg. 9

S2.6 Mean resistivity value of selective non-grave portions of the ERT line pg. 11

S2.7 Analysis of how the resistivity values change with depth pg. 16

S2.8 Resistivity difference plots pg. 21

S3 Soil testing pg. 29

S3.1 Grain size pg. 29

S3.2 Magnetic susceptibility pg. 33

S3.3 Soil water content, organic, and carbonate matter fractions (loss on ignition) pg. 34

S4 References pg. 35

S1 GPR results

S1.1 Velocity analysis

Using the hyperbola fitting tool in ReflexW, the velocity of the hyperbolae indicating PS1 in the one- and 14-month surveys were calculated and found to be 0.09 ns (A in figure S1) and 0.075 ns (B in figure S1), respectively. Due to the extreme homogeneous nature of the soil, only a single layer velocity analysis of each hyperbola was conducted.

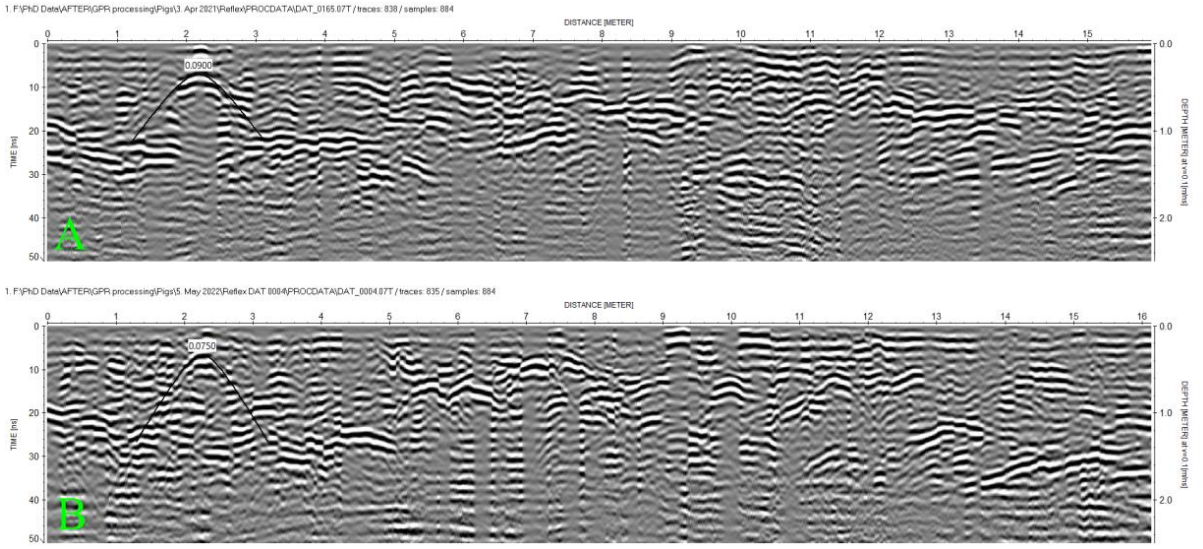


Figure S1. Velocity analysis of the hyperbolae denoting PS1 seen in the one-month (A), and 14-month (B) surveys. GPR profiles were processed, and the hyperbolae were fitted in ReflexW.

S2 ERT Results

To get a deeper understanding of how the resistivity values change throughout the survey period, the mean resistivity values of different parts of the survey area were calculated, which included the pig, fill, whole grave, and whole non-grave areas (see Figure S2). For the purposes of this research, 'pig' is defined as the area where the effects of the pig may be most prevalent, 'fill' is defined as the grave area above the pig, 'whole grave' is the pig, and fill areas combined, and 'whole non-grave' is defined as any area not affected by a grave. As the location of the graves along the ERT line and their depths do not exactly match up with the location of the ERT pegs/cell widths and the depths that the ERT collects data at, the 'whole grave' areas were chosen to the closest cm (see Table S1). The average difference between the grave location and the corresponding ERT pegs are 0.03 m and 0.05 m.

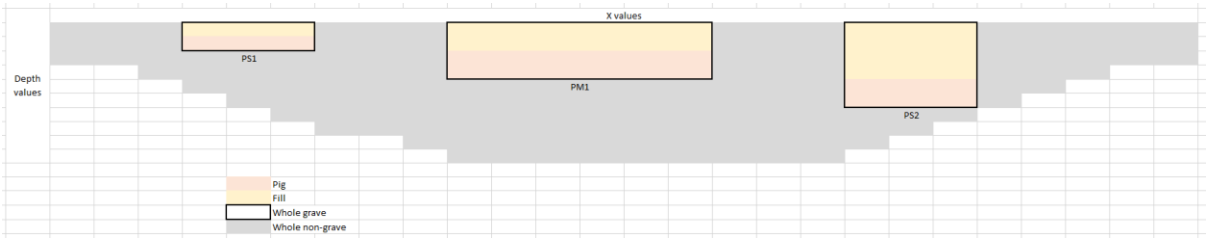


Figure S2. Resistivity value inversion diagrams – visualization of the relevant areas of interest. The mean of each of the above areas were utilized to compare the resistivity values throughout the survey period. Diagram not to scale.

Table S1. Locations of the graves along survey line.

	Location along survey line (m)	Dipole-Dipole			Wenner		
		ERT peg distance (m)	Depth of grave (m)	Depth value from .xyz file (m)	ERT peg distance (m)	Depth of grave (m)	Depth value from .xyz file (m)
Start PS1	1.8	1.812	0.50	0.538	1.875	0.50	0.497
Start PS1 pig	2.05	2.062			2.125		
End PS1 pig	2.36	2.312			2.375		
End PS1	2.77	2.812			2.875		
Start PM1	5.33	5.312	1.0	1.077	5.375	1.0	1.075
Start PM1 pig 1	5.73	5.688			5.625		
End PM1 pig 1	6.12	6.188			6.125		
Start PM1 pig 2	6.36	6.312			6.375		
End PM1 pig 2	6.78	6.812			6.875		
Start PM1 pig 3	7.1	7.062			7.125		
End PM1 pig 3	7.43	7.438			7.375		
End PM1	7.88	7.938			7.875		
Start PS2	9.44	9.438	1.8	1.867	9.375	1.8	1.845
Start PS2 pig	9.7	9.688			9.625		
End PS2 pig	9.93	9.938			9.875		
End PS2 pig	10.34	10.312			10.375		

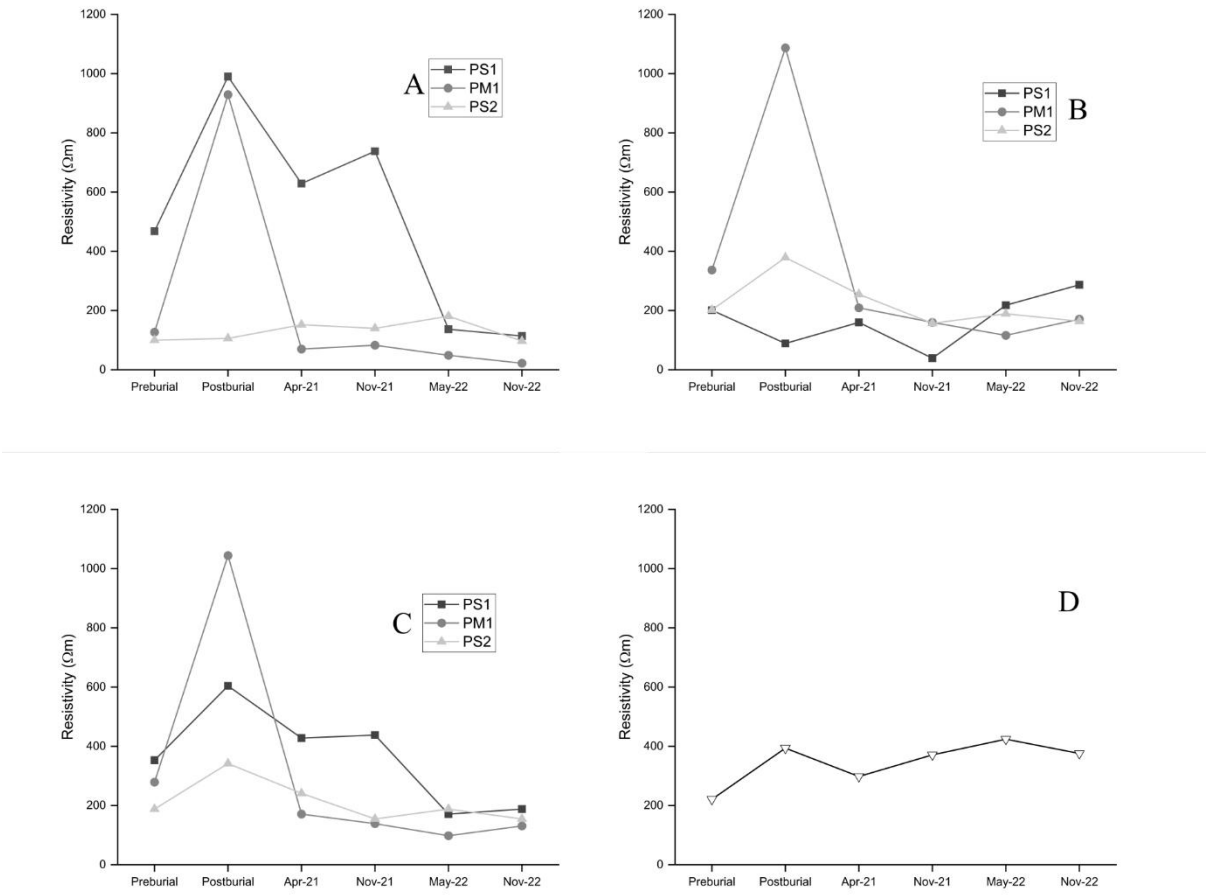


Figure S3. Mean resistivity values for the pig (A), fill (B), whole grave (C), and whole non-grave (D) portions of the ERT line throughout the survey period. Dipole-Dipole array.

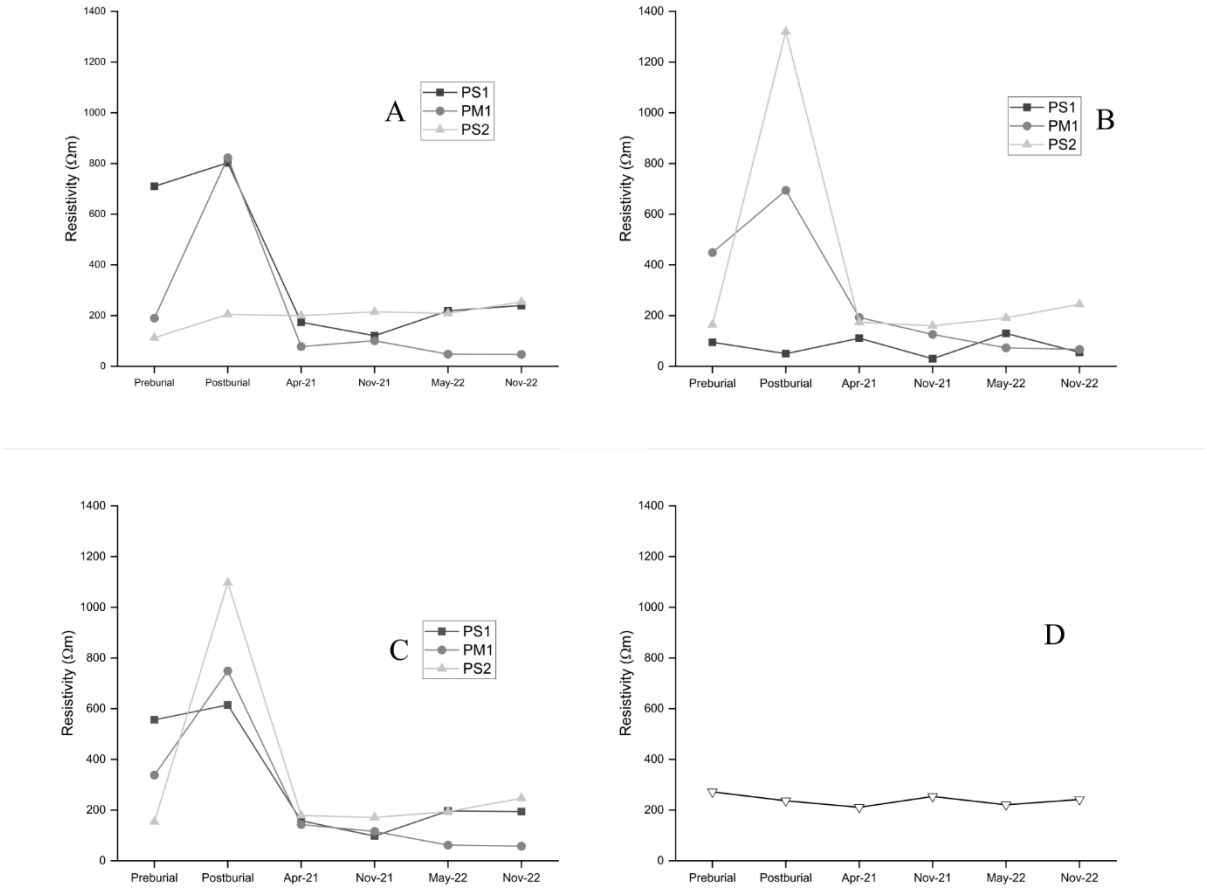


Figure S4. Mean resistivity values for the pig (A), fill (B), whole grave (C), and whole non-grave (D) portions of the ERT line throughout the survey period. Wenner array.

S2.1 Mean resistivity of pig portions of the ERT line

The pig resistivity values are in Figures S3A (Dipole-Dipole) and S4A (Wenner), as well as Table S2. In the Dipole-Dipole data, PS1 has consistently higher values than PM1 and PS2 (except for May-22 where PS2's value is only slightly higher). In the Dipole-Dipole and Wenner data, PS2 has consistently low values – as does PM1, however, in both arrays, PM1 has a high resistivity value at the post-burial survey. In the Wenner data, PS1 also has a high resistivity value at the post-burial survey, however, unlike the Dipole-Dipole data, the pre-burial value is also high.

Table S2. Mean resistivity values of the pig areas.

	Mean resistivity values (Ωm)					
	Dipole-Dipole			Wenner		
	PS1	PM1	PS2	PS1	PM1	PS2
Pre-burial	468	127	100	710	190	113
Post-burial	990	929	106	803	823	205
Apr-21	629	70	152	174	78	200
Nov-21	738	83	140	121	101	215
May-22	137	49	181	219	48	209
Nov-22	114	22	97	240	47	254
Range	854	907	84	682	776	140
Mean	512	213	129	378	215	199

S2.2 Mean resistivity of fill portions of the ERT line

The fill resistivity values are in Figures S3B (Dipole-Dipole) and S4B (Wenner), as well as Table S3. In both the Dipole-Dipole and Wenner arrays, PS1's mean resistivity values do not follow a clear upwards or downwards trend, whereas PM1 and PS2 increase sharply at the post-burial survey before decreasing to the end of the survey.

Table S3. Mean resistivity values of the fill areas.

	Mean resistivity values (Ωm)					
	Dipole-Dipole			Wenner		
	PS1	PM1	PS2	PS1	PM1	PS2
Pre-burial	201	337	202	95	449	164
Post-burial	89	1087	379	50	694	1320
Apr-21	160	209	255	111	193	174
Nov-21	39	160	157	30	126	160
May-22	218	116	189	130	73	191
Nov-22	287	171	164	55	67	245
Range	248	971	222	100	626	1160
Mean	166	347	224	78	267	376

S2.3 Mean resistivity of whole grave portions of the ERT line

The whole grave resistivity values are in Figures S3C (Dipole-Dipole) and S4C (Wenner), as well as Table S4. In the Dipole-Dipole data, PS1 follows no clear upwards or downwards trend, however, despite a high resistivity value at the post-burial survey in PM1, both PM1 and PS2 have consistently low values. In the Wenner data, the three graves follow a similar trend, showing a high resistivity value at the post-burial survey, followed by consistently low resistivity values for the remainder of the survey period. The pre-burial value for the three graves fluctuates, however, are consistently lower than the post-burial survey.

Table S4. Mean resistivity values of the whole grave areas.

	Mean resistivity values (Ωm)					
	Dipole-Dipole			**Wenner**		
	PS1	**PM1**	**PS2**	**PS1**	**PM1**	**PS2**
Pre-burial	353	279	188	556	338	154
Post-burial	604	1044	342	615	749	1097
Apr-21	428	171	241	158	143	179
Nov-21	438	139	155	98	116	171
May-22	171	98	188	197	62	194
Nov-22	188	131	155	194	58	247
Range	433	946	187	517	691	943
Average	364	310	212	303	245	340

The cumulative rainfall and average soil moisture percentages were graphed against the whole grave values of PS1, PM1, and PS2, and the results can be found in Figures S5 (Dipole-Dipole) and S6 (Wenner).

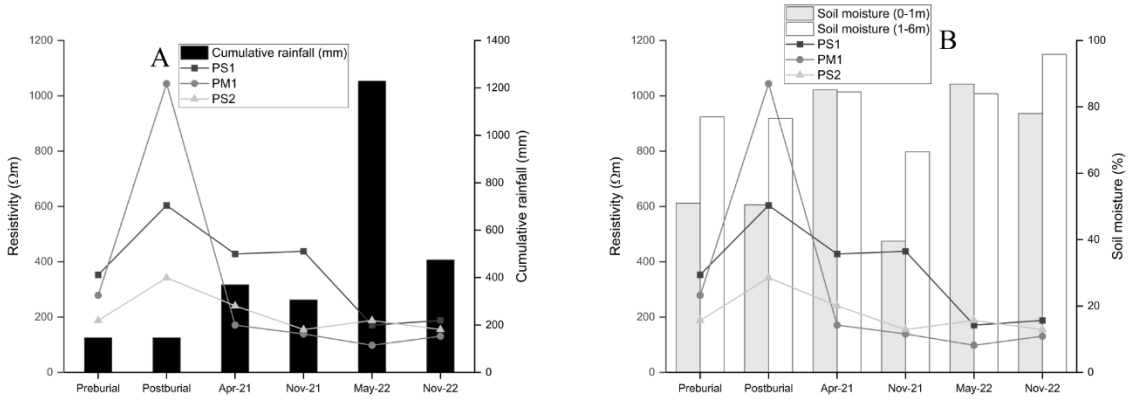


Figure S5. Comparing the whole grave resistivity values of PS1, PM1, and PS2 to A) cumulative rainfall and B)

shallow (0-1 m) and deep (1-6 m) soil moisture percentages. Dipole-Dipole data. The rainfall and soil moisture data were sourced from The Bureau of Meteorology.

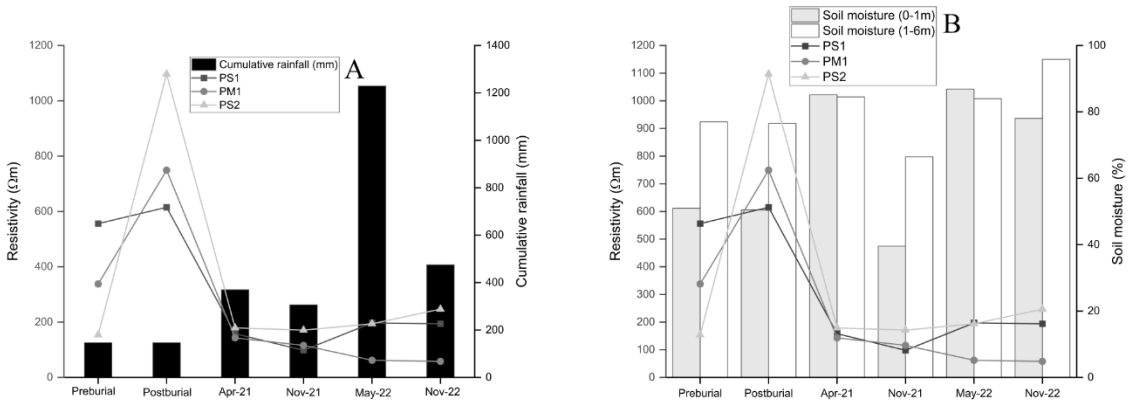


Figure S6. Comparing the whole grave resistivity values of PS1, PM1, and PS2 to A) cumulative rainfall and B) shallow (0-1 m) and deep (1-6 m) soil moisture percentages. Wenner data. The rainfall and soil moisture data were sourced from The Bureau of Meteorology.

S2.4 Mean resistivity of whole non-grave portions of the ERT line

To better understand the resistivity changes of the graves, the non-grave area was assessed, with the idea that any differences seen in the non-grave areas can be removed as a possible reason for the changes seen in the grave areas. To accomplish this, the grave-related values were removed, and the remainder of the values were averaged. The whole non-grave resistivity values are in Figures S3D (Dipole-Dipole) and S4D (Wenner), as well as Table S5.

Table S5. Mean resistivity values of the whole non-grave area.

	Mean resistivity values (Ωm)	
	Dipole-Dipole	**Wenner**
Pre-burial	221	272
Post-burial	394	237
Apr-21	298	211
Nov-21	371	254
May-22	424	221
Nov-22	376	242
Range	203	61
Mean	347	240

The whole non-grave values were graphed against the cumulative rainfall and average soil moisture, as shown in Figures S7 (Dipole-Dipole) and S8 (Wenner).

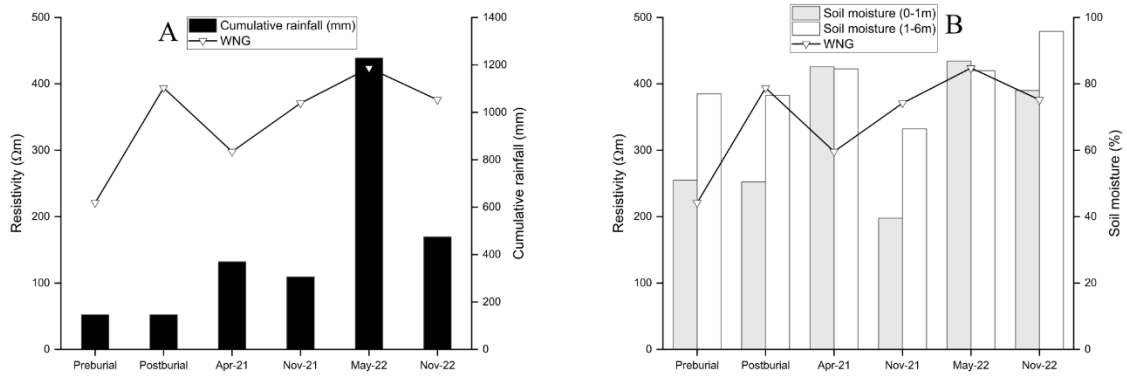


Figure S7. Comparing the resistivity values of the whole non-grave area to A) cumulative rainfall and B) shallow (0-1 m) and deep (1-6 m) soil moisture percentages. Dipole-Dipole data. The rainfall and soil moisture data were sourced from The Bureau of Meteorology.

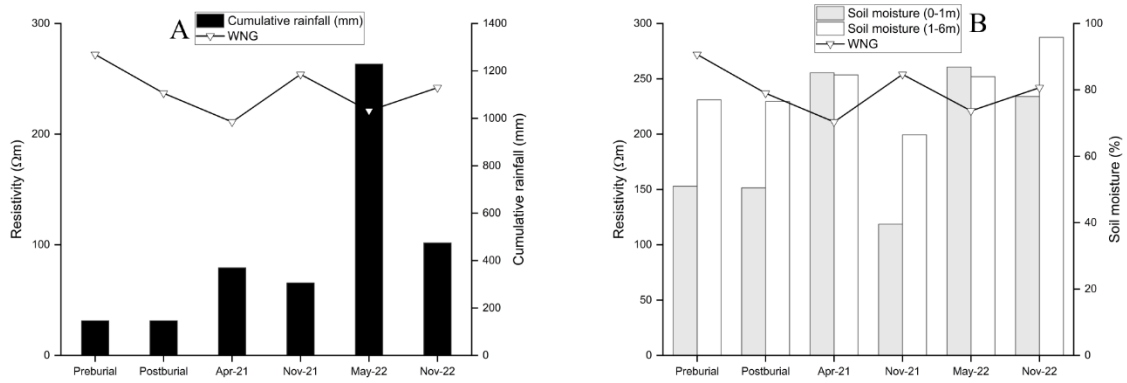


Figure S8. Comparing the resistivity values of the whole non-grave area to A) cumulative rainfall and B) shallow (0-1 m) and deep (1- 6m) soil moisture percentages. Wenner data. The rainfall and soil moisture data were sourced from The Bureau of Meteorology.

S2.5 Comparing the mean resistivity value of whole grave and whole non-grave portions of the ERT line

To better understand how the cadavers affected the resulting resistivity values, the whole grave and whole non-grave values were compared – the results can be seen in Figures S9 (Dipole-Dipole) and S10 (Wenner) and Table S6.

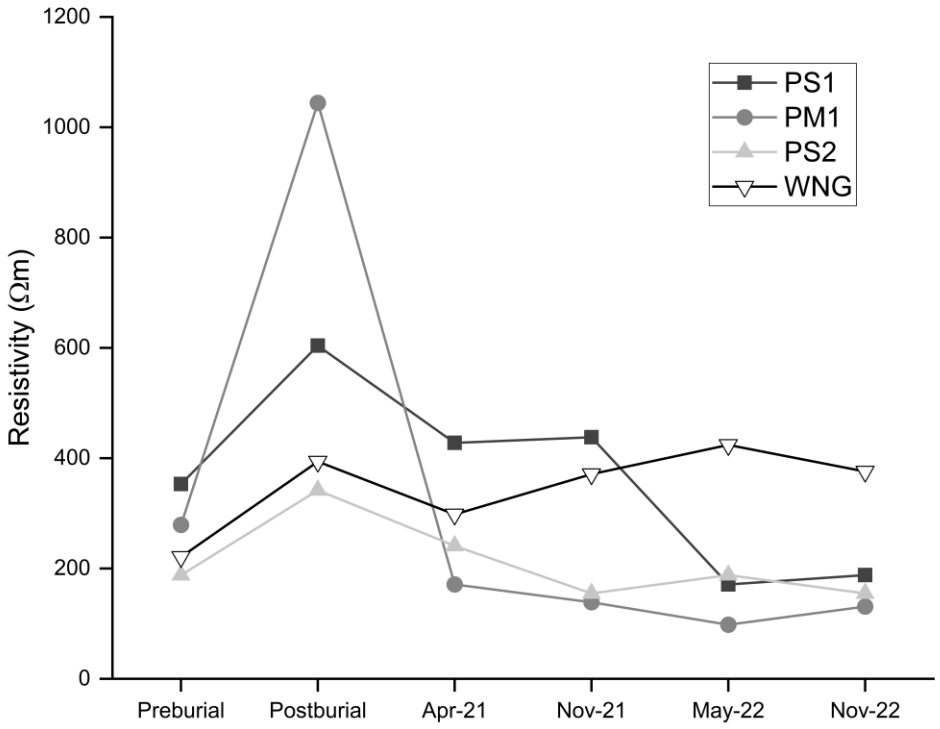


Figure S9. Comparison between the whole grave resistivity values of PS1, PM1, and PS2 and the whole non-grave (WNG) resistivity values. Dipole-Dipole array.

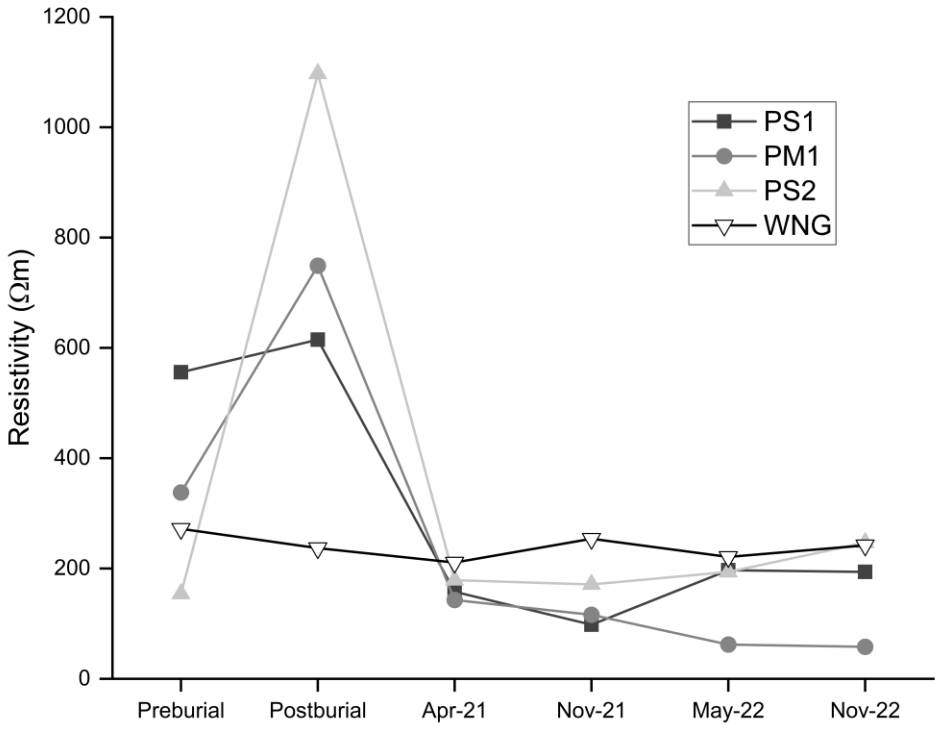


Figure S10. Comparison between the whole grave resistivity values of PS1, PM1, and PS2 and the whole non-grave (WNG) resistivity values. Wenner array.

Table S6. Percentage differences in mean resistivity values of the whole grave and whole non-grave areas.

	Percentage differences in resistivity values (%)					
	Dipole-Dipole			**Wenner**		
	PS1vWNG	**PM1vWNG**	**PS2vWNG**	**PS1vWNG**	**PM1vWNG**	**PS2vWNG**
Pre-burial	60	26	-15	105	24	-43
Post-burial	53	165	-13	160	216	363
Apr-21	44	-43	-19	-25	-32	-15
Nov-21	18	-63	-58	-61	-55	-33
May-22	-60	-77	-56	-11	-72	-12
Nov-22	-50	-65	-59	-20	-76	2
Sum	284	438	220	382	475	469
Mean	47	73	37	64	79	78

The percentage differences were calculated with the following equation: $\left(\frac{\text{Whole grave}-\text{Whole non}-\text{grave}}{\text{Whole non}-\text{grave}}\right) * 100$

S2.6 Mean resistivity value of selective non-grave portions of the ERT line

When averaging a large number of values, which is the case in the whole non-grave mean calculation, the variability of the dataset gets diminished. To account for this, the whole non-grave area was divided into seven different areas, and the resistivity values were averaged. By following Figure S11, the following areas were selected for further analysis:

- Pre PS1 (all resistivity values from the start of the line to PS1)
- Under PS1 (all resistivity values under PS1)
- PS1-PM1 (all resistivity values in between PS1 and PM1)
- Under PM1 (all resistivity values under PM1)
- PM1-PS2 (all resistivity values between PM1 and PS2)
- Under PS2 (all resistivity values under PS2)
- Post PS2 (all resistivity values after PS2 until the end of the line)

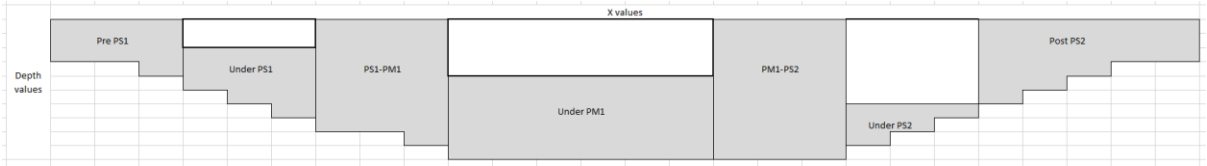


Figure S11. Resistivity inversion diagram denoting the selective non-grave areas for further analysis. Diagram not to scale.

The mean resistivity areas from each of the selective non-grave areas were graphed against the cumulative rainfall and soil moisture and can be found in Figures S12 and S13 (Dipole-Dipole) and S14 and S15 (Wenner). Although it is well-known that resistivity values will highly vary, even in a homogenous area, it is interesting that there are no consistent trends in any of the non-grave areas. With the exception of under PM1, PM1-PS2, and under PS2 for both arrays, which are all on the SW end of the study site and have a similar pattern and peak at the 14-month survey, the other areas all seem to peak at different times. Despite a similar pattern with three of the areas on the SW end of the site, post PS2, which is the most SW part of the site, does not follow the pattern.

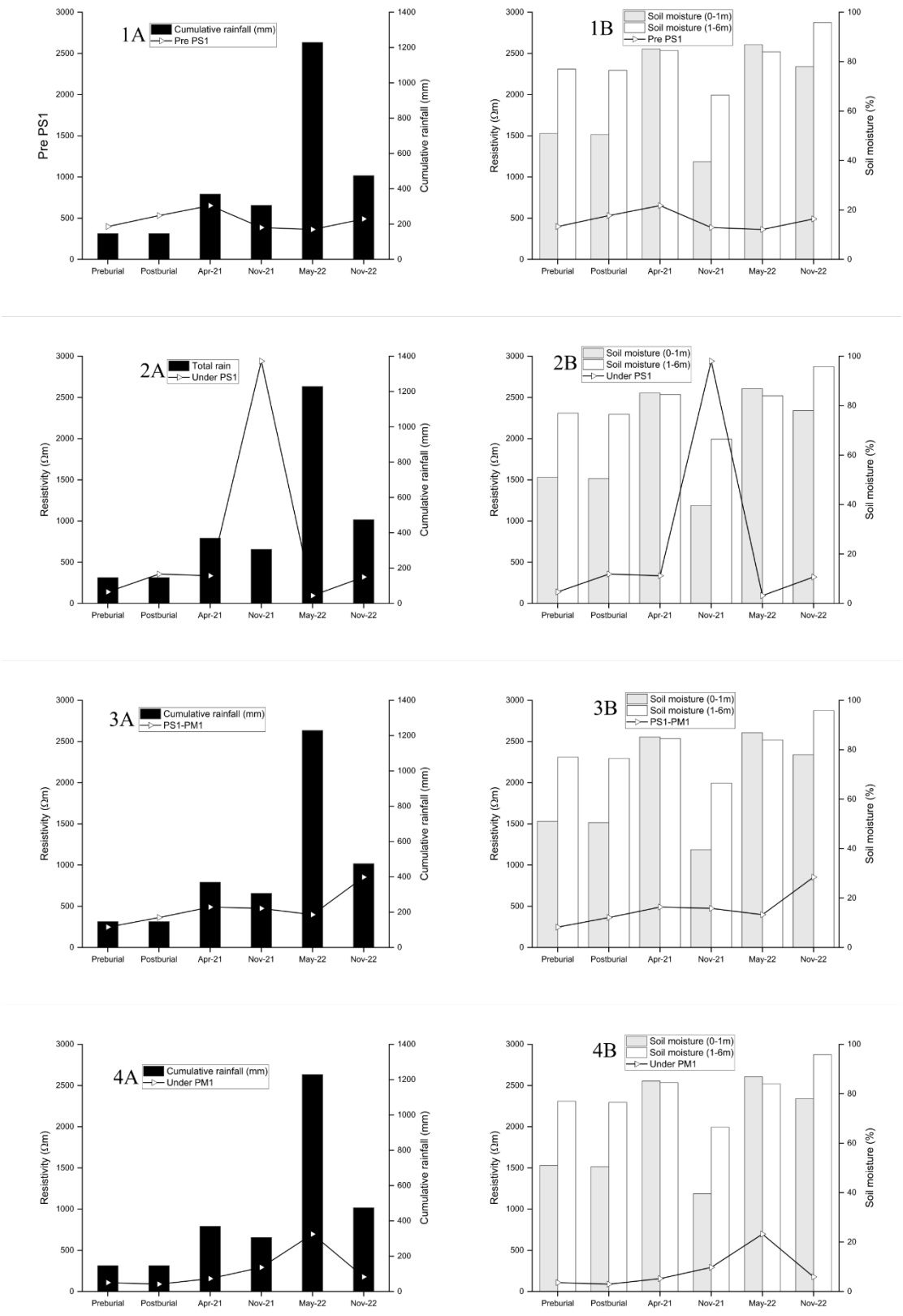


Figure S12. Selective non-grave areas, including Pre PS1 (1), Under PS1 (2), PS1-PM1 (2), and Under PM1 (4), graphed against the cumulative rainfall (A) and the soil moisture data (B). Dipole-Dipole data. Both the rainfall and soil moisture data were sourced from The Bureau of Meteorology.

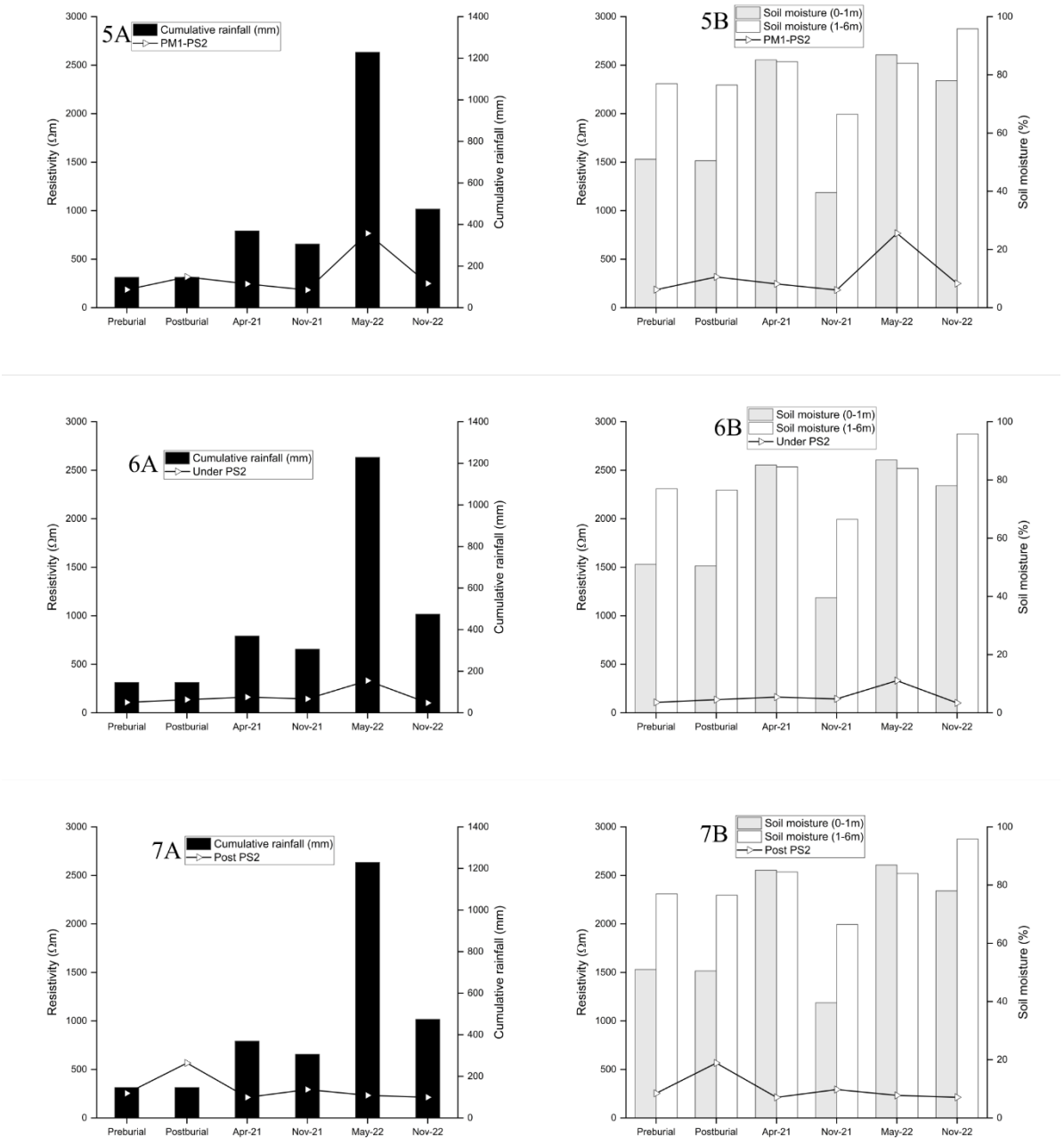


Figure S13. Selective non-grave areas, including PM1-PS2 (5), Under PS2 (6), and Post PS2 (7), graphed against the cumulative rainfall (A) and the soil moisture data (B). Dipole-Dipole data. Both the rainfall and soil moisture data were sourced from The Bureau of Meteorology.

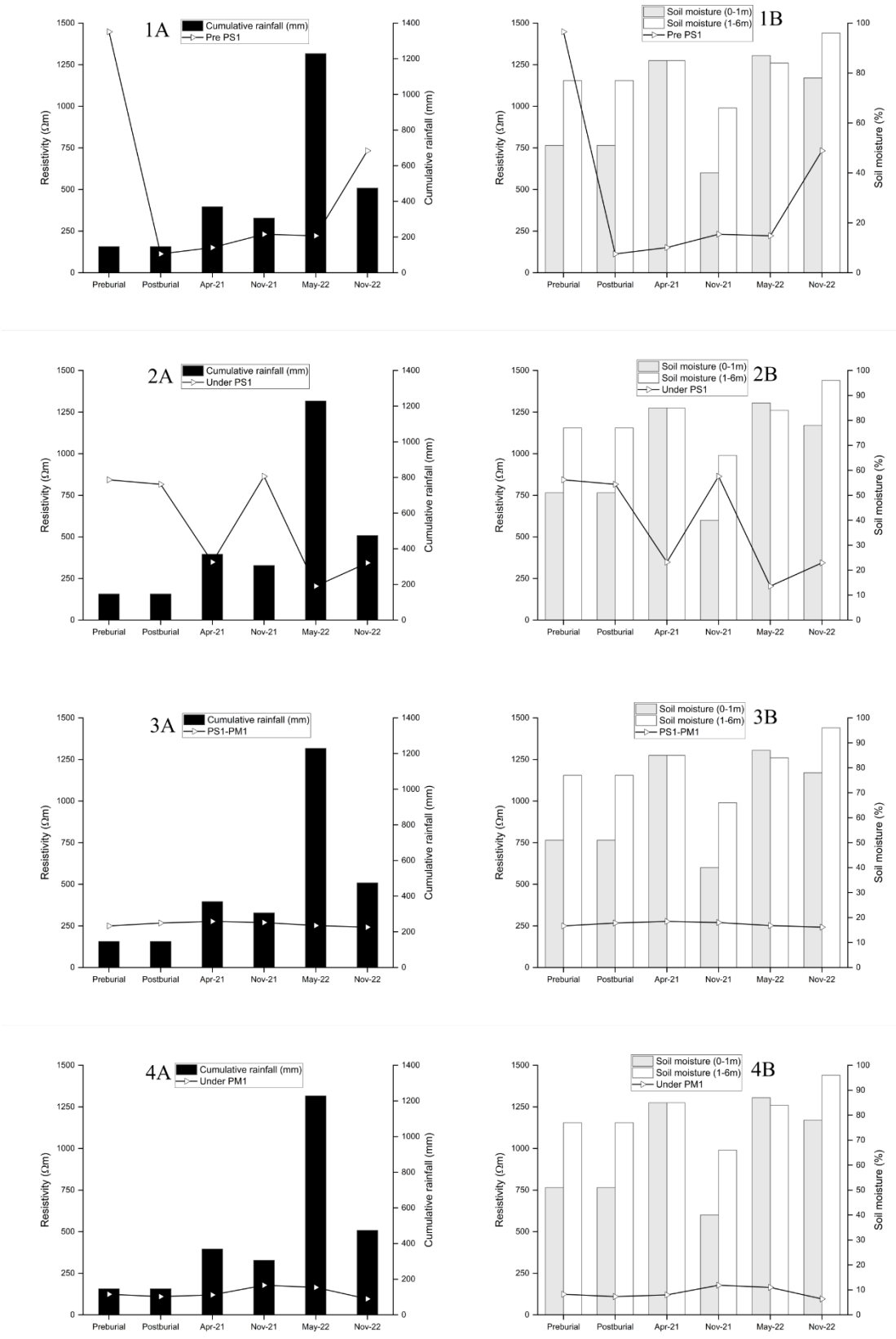


Figure S14. Selective non-grave areas, including Pre PS1 (1), Under PS1 (2), PS1-PM1 (2), and Under PM1 (4), graphed against the cumulative rainfall (A) and the soil moisture data (B). Wenner data. Both the rainfall and soil moisture data were sourced from The Bureau of Meteorology.

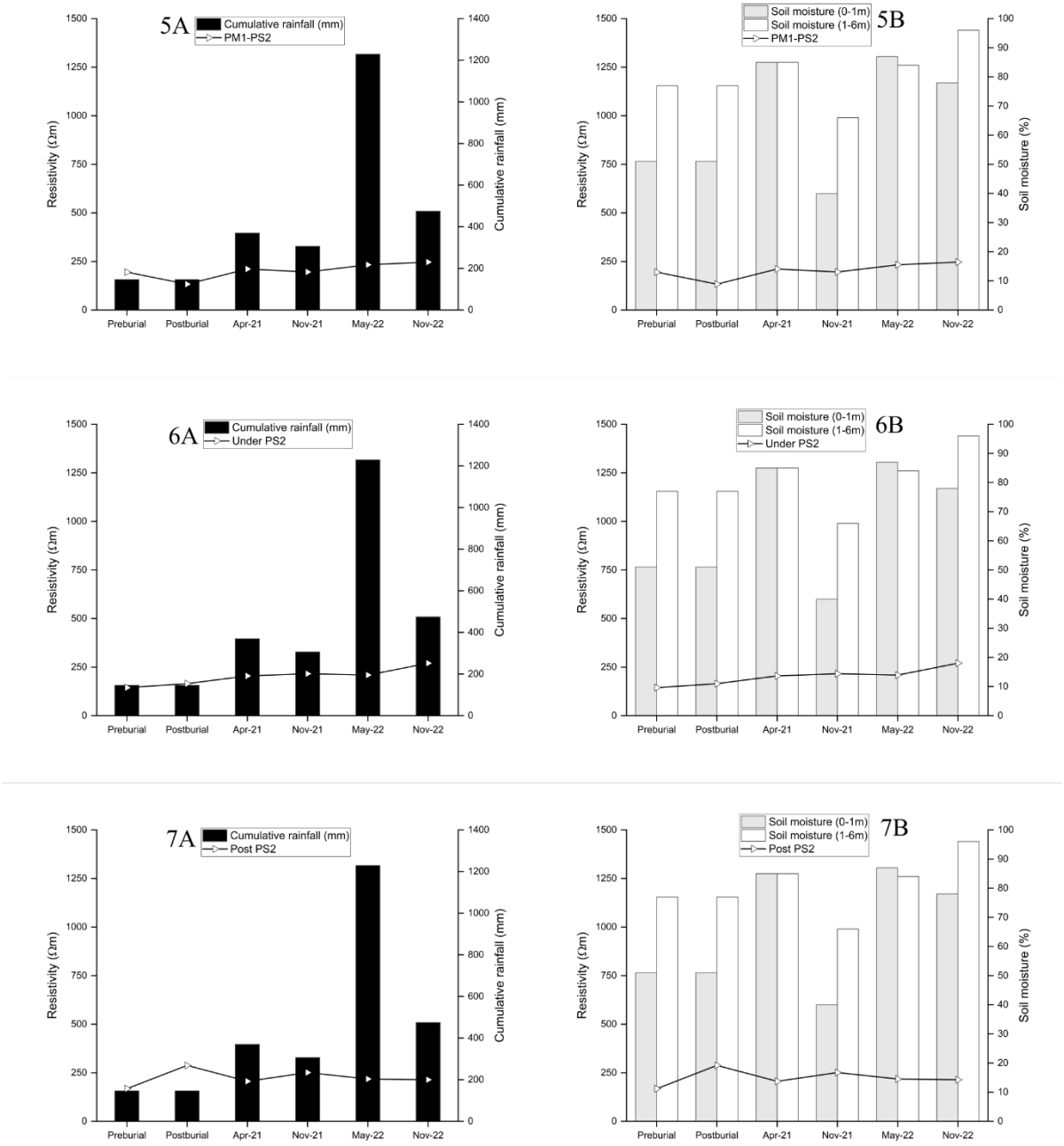


Figure S15. Selective non-grave areas, including PM1-PS2 (5), Under PS2 (6), and Post PS2 (7), graphed against the cumulative rainfall (A) and the soil moisture data (B). Wenner data. Both the rainfall and soil moisture data were sourced from The Bureau of Meteorology.

S2.7 Analysis of how the resistivity values change with depth

To analyse how the pig cadavers and depth affect the resistivity values, five vertical transects along the ERT line values were chosen, including three in the middle of each of the graves and two in non-grave areas between PS1/PM1 and PM1/PS2, and the resistivity values from the surface to the deepest point were compared. The selected areas can be

visualized in figure S16. For the Dipole-Dipole array, the PS1 values were taken at 2.188 m, the PM1 values were calculated by averaging the values at 5.938 m, 6.562 m, and 7.188 m (mid points of each of the pig cadavers), and the PS2 values were taken at 9.812 m. Additionally, the non-grave values were taken at 4.188 m and 8.688 m. For the Wenner array, the PS1 values were taken at 2.375 m, the PM1 values were calculated by averaging the values at 5.875 m, 6.625 m, and 7.125 m (mid points of each of the pig cadavers), and the PS2 values were taken at 9.625 m. Additionally, the non-grave values were taken at 4.125 m and 8.625 m. These values are the distance along the line from the start of the line.

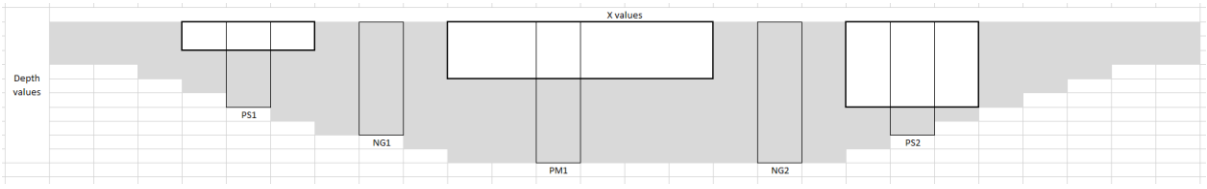
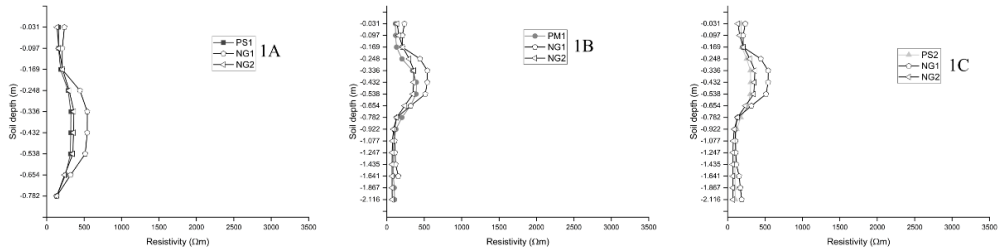


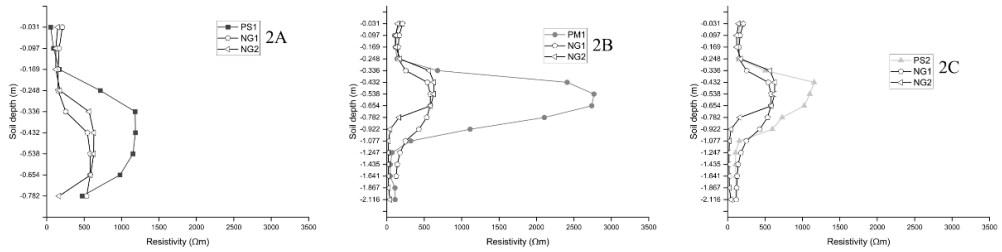
Figure S16. Resistivity value inversion diagram denoting the change with depth measurements through the midpoint of PS1, PM1, and PS2, as well as two non-grave areas. Diagram not to scale.

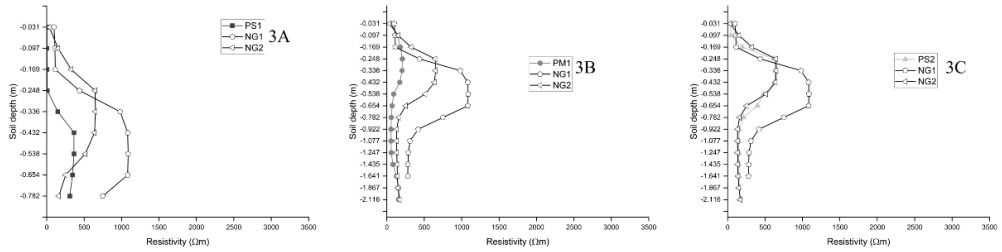
As shown in Figure S16, the changes in the resistivity values with depth were examined for the three graves, as well as two non-grave areas. The results can be found in Figures S17 (Dipole-Dipole) and S18 (Wenner). The graphs can be used to examine the individual patterns of the grave and non-grave areas, as well as to compare the grave and non-grave areas (for the latter, refer to the discussion in the main text). Firstly, when looking at the changes with depth in the grave areas individually, the most common trend in the Dipole-Dipole data is low resistivity values from the surface to ~0.169 m deep, a peak from ~0.169 m to ~0.782 m deep, and then consistently low resistivity values to the deepest point (0.782 m deep for PS1 and then 2.116 m deep for PM1 and PS2). This trend is not seen in the one-month and eight-month surveys of PS1 (Figure S17-3A and -4A), where the resistivity values are consistently low until 0.248-0.336 m deep, and then increase to the deepest point. The increase in these two surveys is significantly larger in the eight-month survey of PS1. The other two surveys that do not fit the trend are the 14-month survey of PM1 (Figure S17-5B) and the 20-month survey of PS1 (Figure S17-6A), where there is a small increase in the first 30 cm, followed by consistently low resistivity values until the deepest point, where the resistivity increases again. In the Wenner data, the most common trend is low resistivity values at the surface, an increase around 0.497 m deep, and then plateaued values to the

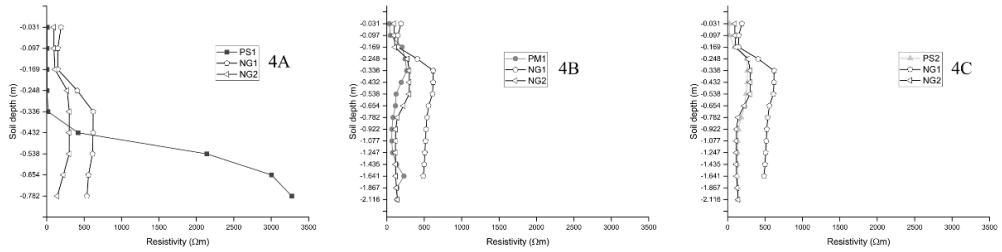
deepest point. The pre-burial surveys of PM1 (Figure S18-1B) and PS2 (Figure S18-1C) and the three post-burial surveys (Figure S18-2A, 2B, and 2C) are similar to the Dipole-Dipole trend with low initial values, an increase from 20-80 cm deep, and then low values to the deepest point. The eight-month (Figure S18-3B), 14-month (Figure S18-4B), and 20-month (Figure S18-6B) PM1 surveys follow this trend as well except for a small increase at the deepest point of the survey. Finally, the 14-month survey of PM1 and the 20-month survey of PS1 follow their own trend that includes consistently low resistivity values, with an increase and plateau towards the deeper points.

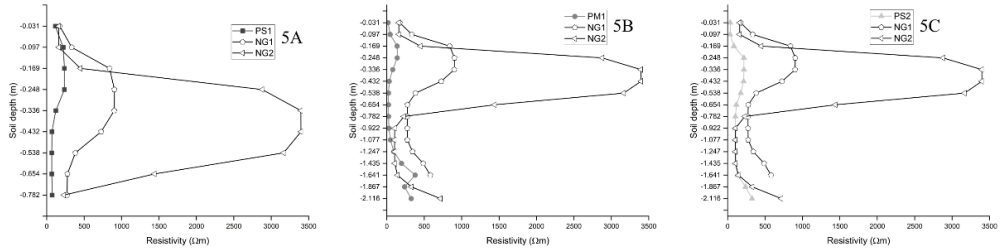
Next, for the Dipole-Dipole data, the non-grave areas follow two main trends; 1) initially low resistivity values, a peak from ~20 cm to ~1 m deep, followed by low resistivity values to the deepest point, which can be seen in the three pre-burial surveys (Figure S17-1A-C), the post-burial and one-month surveys for PM1 (Figure S17-2B and 3B) and PS2 (Figure S17-2C and 3C), and the three 14-month surveys (Figure S17-5A-C), and 2) initially low resistivity values, a peak at ~20 m deep, followed by plateaued values until the deepest point of the survey, which can be seen in the remainder of the surveys. For the Wenner data, there are three main trends; 1) low resistivity values at the surface, followed by an sudden increase to ~1 m deep, and then consistently low values to the deepest point, which can be seen in the three pre-burial surveys (Figure S18-1A-C), 2) initially low resistivity values, a peak ~20 cm to ~1 m deep, followed by low resistivity values to the deepest point, which can be seen in the three surveys for the one-, 14- and 20-month surveys (Figure S18-2A-C, 5A-C, and 6A-C), and 3) an initial decrease in the first 20 cm, followed by an increase and a plateau of values until the deepest point, which can be seen in the remainder of the surveys.


PS1
NG1
NG2
1A
PM1
NG1
NG2
1B
PS2
NG1
NG2
1C
Soil depth (m)
Resistivity (Ωm)


PS1
NG1
NG2
2A
PM1
NG1
NG2
2B
PS2
NG1
NG2
2C
Soil depth (m)
Resistivity (Ωm)


PS1
NG1
NG2
3A
PM1
NG1
NG2
3B
PS2
NG1
NG2
3C
Soil depth (m)
Resistivity (Ωm)


PS1
NG1
NG2
4A
PM1
NG1
NG2
4B
PS2
NG1
NG2
4C
Soil depth (m)
Resistivity (Ωm)


PS1
NG1
NG2
5A
PM1
NG1
NG2
5B
PS2
NG1
NG2
5C
Soil depth (m)
Resistivity (Ωm)

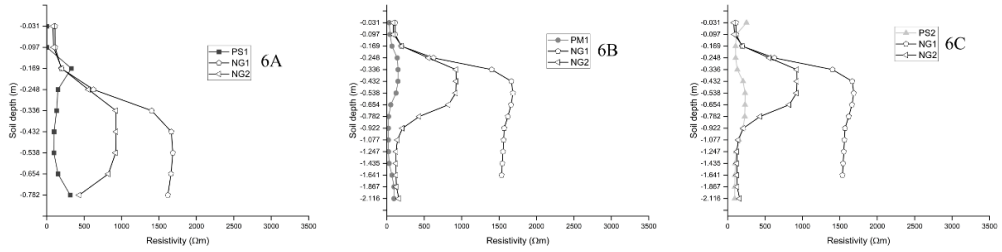

PS1
NG1
NG2
6A
PM1
NG1
NG2
6B
PS2
NG1
NG2
6C
Soil depth (m)
Resistivity (Ωm)

Figure S17. Changes in the resistivity values with depth of the grave and non-grave areas. 1) pre-burial, 2) post-burial, 3) Apr-21, 4) Nov-21, 5) May-22, and 6) Nov-22. A) PS1, B) PM1, and C) PS2. Dipole-Dipole data.

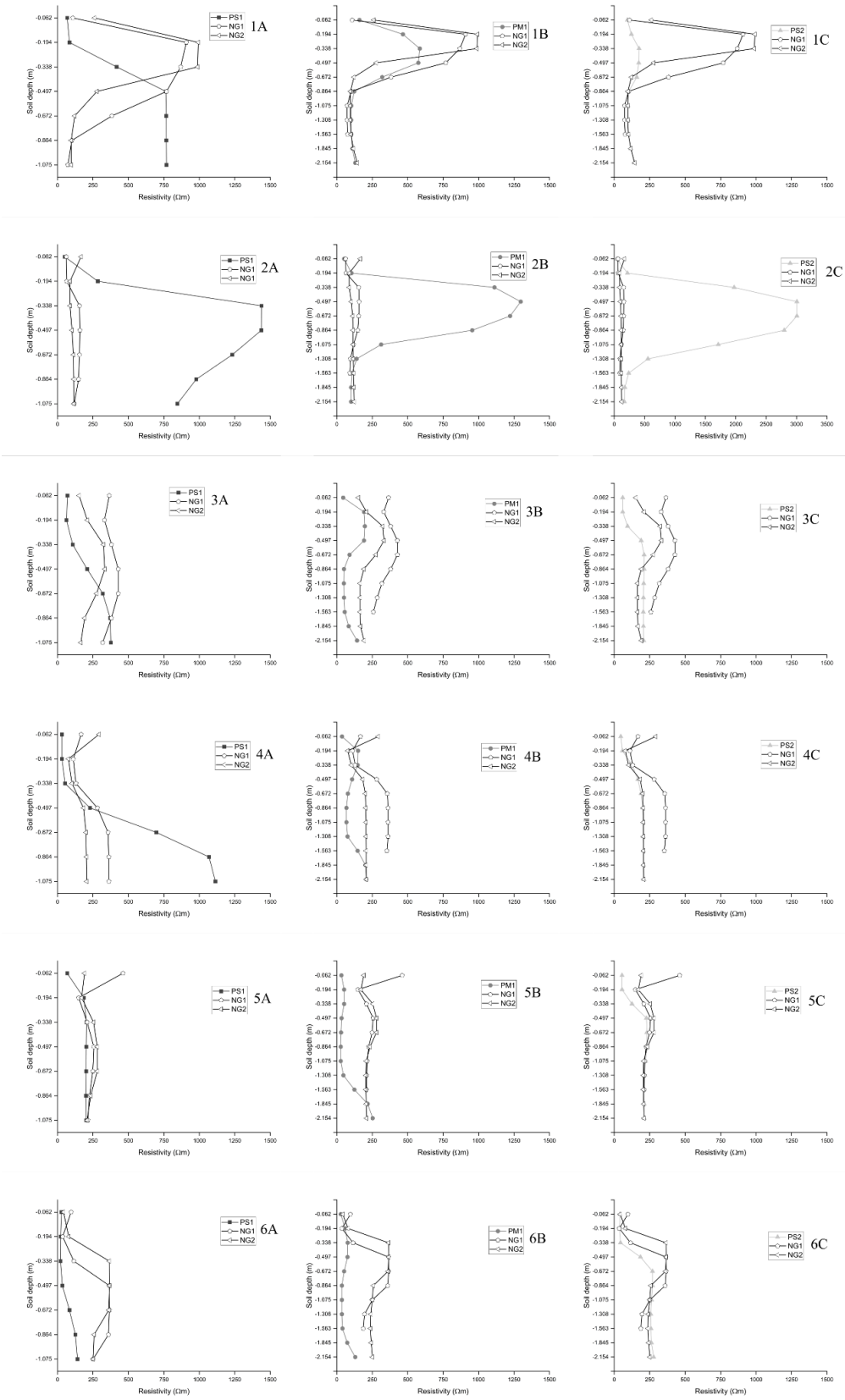


Figure S18. Changes in the resistivity values with depth of the grave and non-grave areas. 1) pre-burial, 2) post-burial, 3) Apr-21, 4) Nov-21, 5) May-22, and 6) Nov-22. A) PS1, B) PM1, and C) PS2. Please note the scale difference in 2C, as there were some resistivity values well above 1500, however, homogenizing the rest of the profiles to a 3000 Ωm scale would cause a loss of trend visibility. Wenner data.

S2.8 Resistivity difference plots

To further understand the resistivity differences throughout the survey period, resistivity difference plots were created for all combinations of surveys. With the pre-burial survey acting as a control, the subsequent five surveys were compared to the to see how the resistivity values changed, based on the presence of the cadaver, as well as the rainfall and soil moisture. In the Dipole-Dipole data (Figure S19), the largest changes in resistivity from the pre-burial survey are seen in the 14- (Figure S19d) and 20-month (Figure S19e) surveys. When comparing the one-month (Figure S19b), and all subsequent surveys (Figure S19c-e), to the pre-burial survey, PS1 and PM1 show the largest change in resistivity, indicated by a low resistivity change, while PS2 is largely unchanged (with slight increases and decreases throughout the survey period). Additionally, the non-grave areas are mostly highlighted by a resistivity increase, with slight resistivity decreases at the SW end of the survey line. When using the post-burial survey as the control, the subsequent four surveys were compared (Figure S20f-i) which showed no obvious changes in the non-grave areas, however, there are resistivity decreases in PS1, PM1, and PS2. When using the one-month survey as a control, the subsequent three surveys were compared (Figure S21j-l). The grave areas are highlighted by a resistivity decrease, while the surrounding areas are a mixture of resistivity increases (under PS1 in j, under PM1 in k, and between PS1 and PM1 in l), and resistivity decreases (from approximately 0.5 m to 1.5 m deep across the survey). When using the eight-month survey as a control, the comparison between the 14-month survey (Figure S21m) shows that PS1 is highlighted by a resistivity increase, PM1 is highlighted by a resistivity decrease, PS2 is largely unchanged (with a small resistivity increase in the SW wall approximately 0.5 m deep), and the non-grave areas highlight resistivity decreases down to 2 m deep across the survey, and then a resistivity increase deeper than 2 m. The comparison between the 20-month survey (Figure S21n) shows a similar trend in the grave areas of the eight- and 14-month comparisons, however, the non-grave areas are mostly highlighted by a resistivity decrease, except for a resistivity increase between PS1 and PM1. Finally, the comparison

between the 14- and 20-month surveys (Figure S21o) shows that the grave areas are mostly unchanged, except for small increases and decreases on the grave walls, however, the non-grave areas show a mixture or increases (between PS1 and PM1) and decreases (deeper than 2 m).

In the Wenner data, when using the pre-burial survey as a control (Figure S22a-e), the non-grave areas are largely unchanged, with the grave areas being highlighted by a resistivity decrease (except for the increase seen when comparing pre- and post-burial – Figure S22a). When using the post-burial survey as a control (Figure S23f-i), the non-grave areas are highlighted by a slight resistivity increase with the grave areas being highlighted by clear resistivity decreases. When using the one-month survey as a control (Figure S24j-l), the shallow depths (up to 1 m) are highlighted by a resistivity decrease, with the deeper areas highlighted as a resistivity decrease (except for the one- and 20-month comparison where the resistivity increase is on and under PS2). Additionally, PS1 and PS2 are highlighted by a resistivity increase while PM1 is highlighted by a resistivity decrease. When using the eight-month survey as a control (Figure S24m-n), PS1 and PS2 are highlighted by a resistivity increase, PM1 is highlighted by a resistivity decrease, and the surrounding non-grave areas are mostly indicated by a resistivity decrease (except for under PS1 and PS2, which shows a resistivity increase). Finally, in the 14- and 20-month survey comparison (Figure S24o), the changes in the non-grave areas are similar to the eight- and 14-month comparison, with PS1 showing a resistivity decrease, and then PM1 and PS2 as resistivity increases.

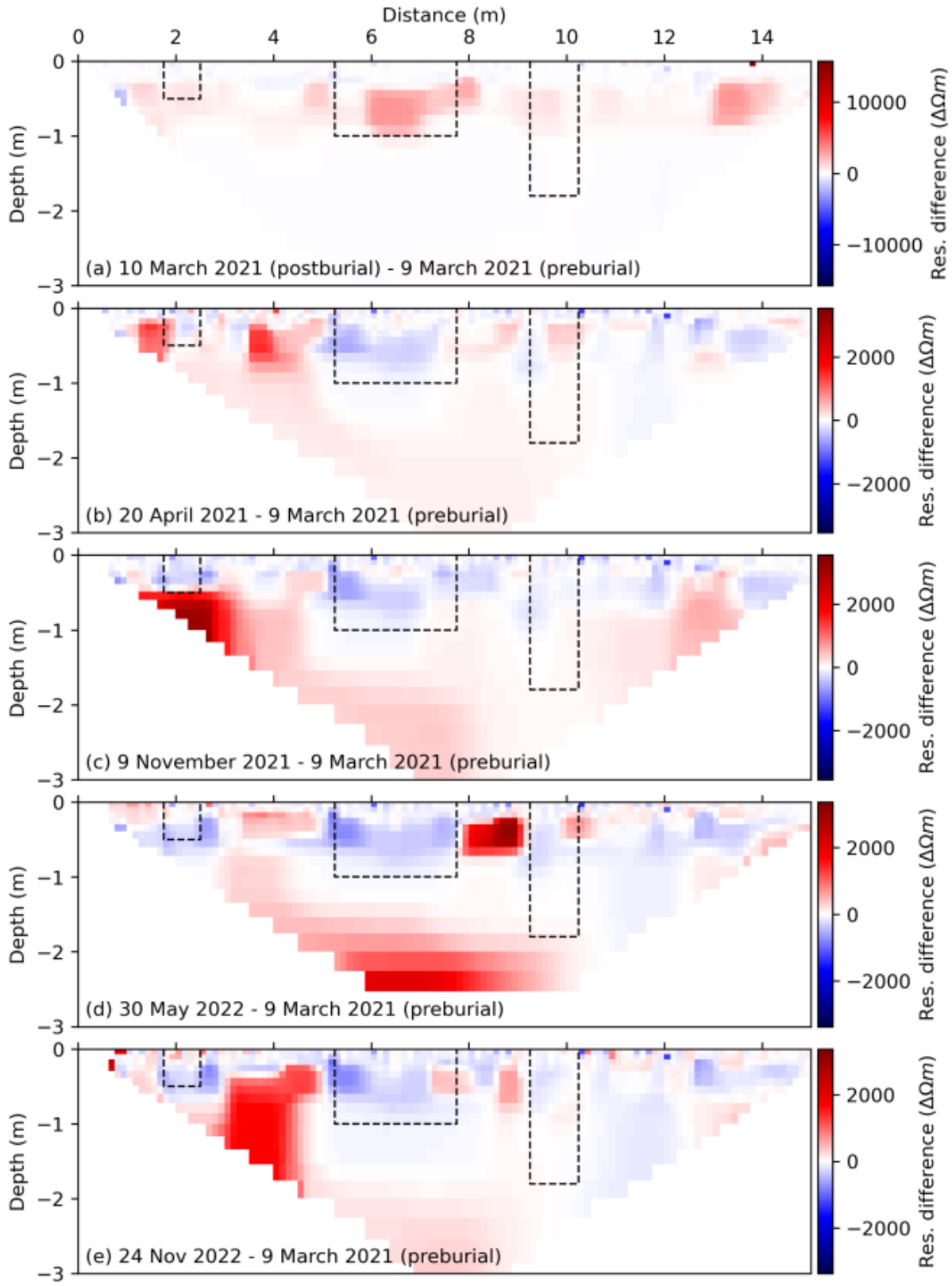


Figure S19. Resistivity difference plots between a) post-burial and pre-burial, b) Apr-21 and pre-burial, c) Nov-21 and pre-burial, d) May-22 and pre-burial, and e) Nov-22 and pre-burial. Red represents an increase and blue represents a decrease in resistivity between two surveys. Dipole-Dipole data. Difference plots were generated in Python.

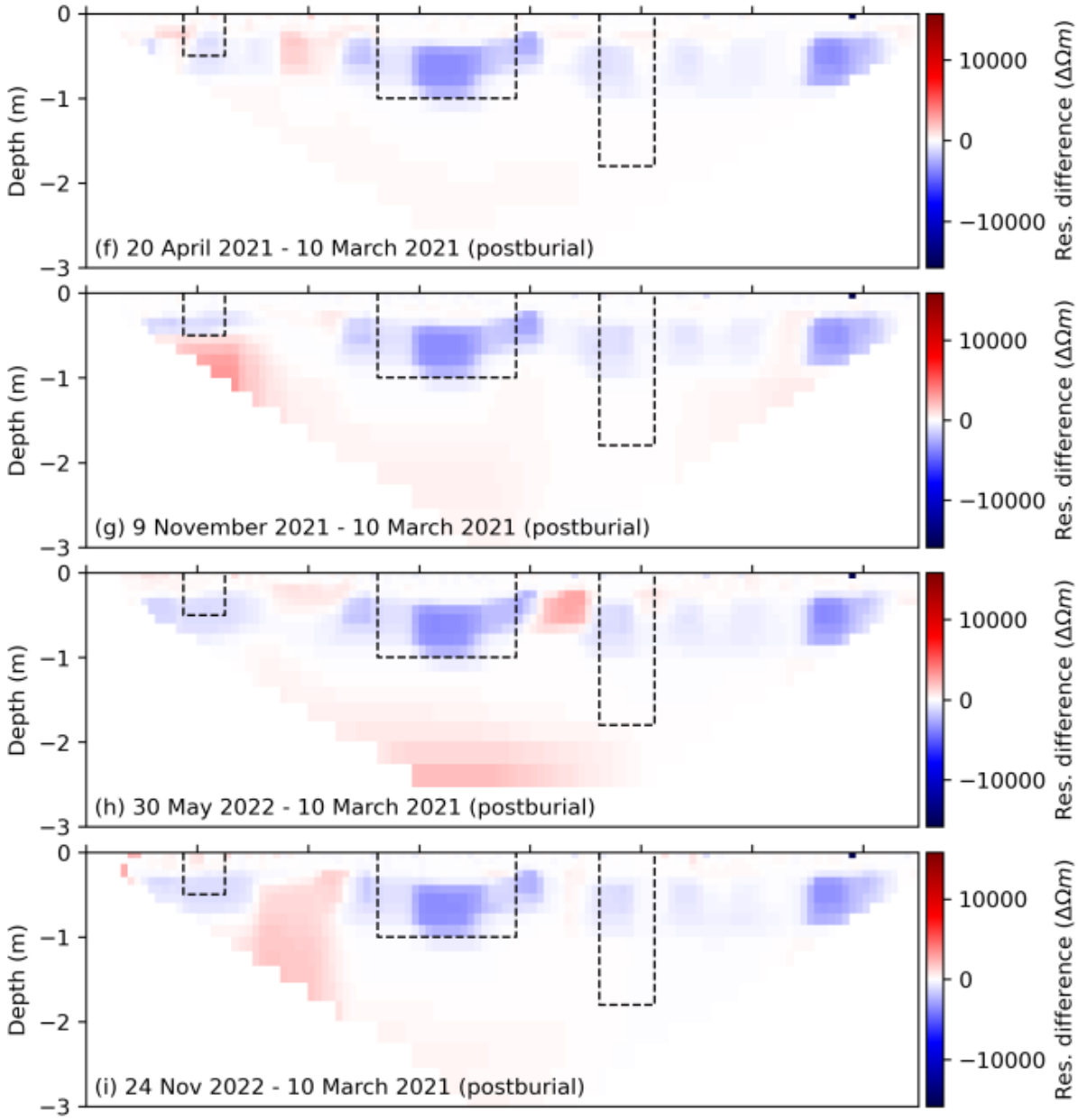


Figure S20. Resistivity difference plots between f) Apr-21 and post-burial, g) Nov-21 and post-burial, h) May-22 and post-burial, and i) Nov-22 and post-burial. Red represents an increase and blue represents a decrease in resistivity between two surveys. Dipole-Dipole data. Difference plots were generated in Python.

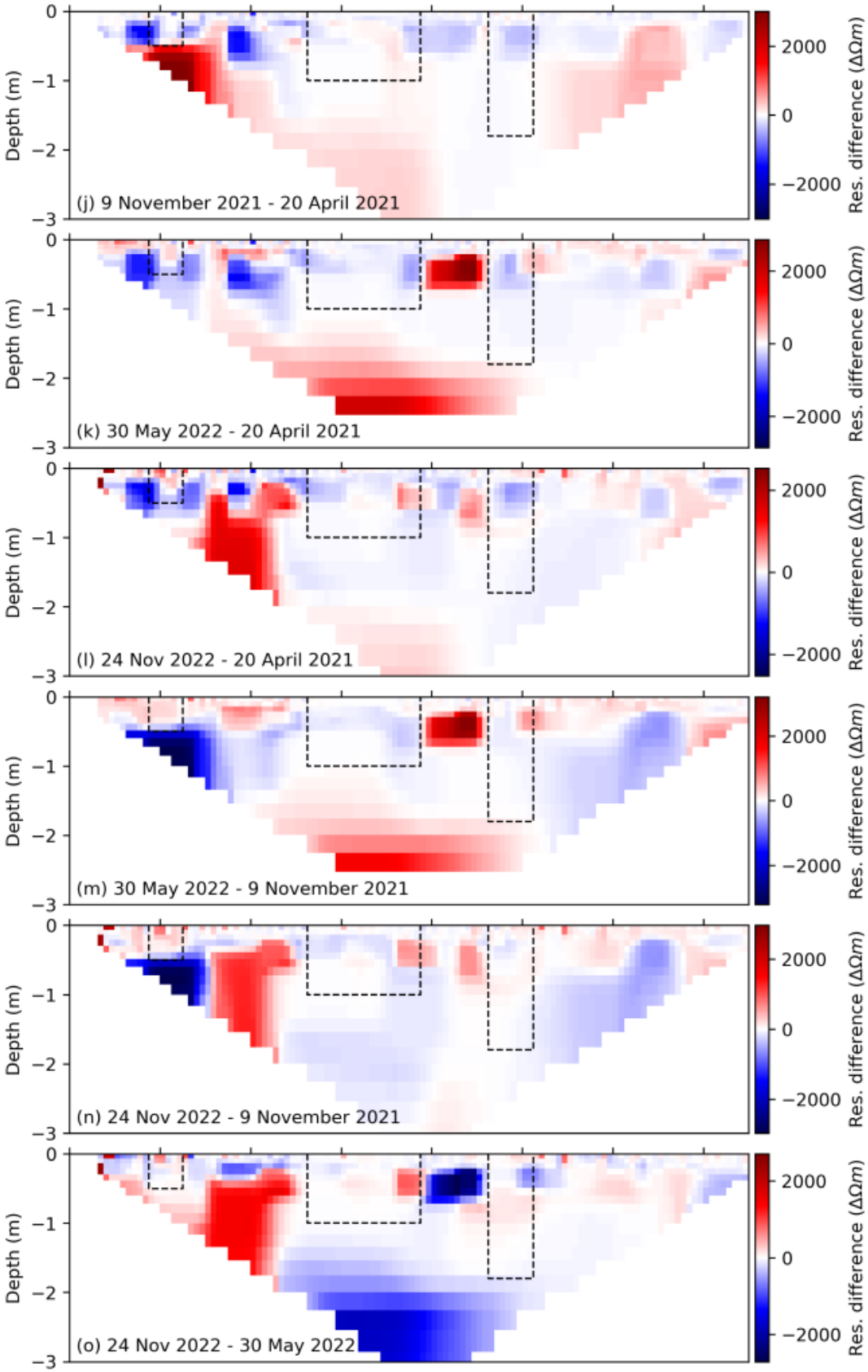


Figure S21. Resistivity difference plots between j) Nov-21 and Apr-21, k) May-22 and Apr-21, l) Nov-22 and Apr-21, m) May-22 and Nov-21, n) Nov-22 and Nov-21, and o) Nov-22 and May-22. Red represents an increase and

blue represents a decrease in resistivity between two surveys. Dipole-Dipole data. Difference plots were generated in Python.

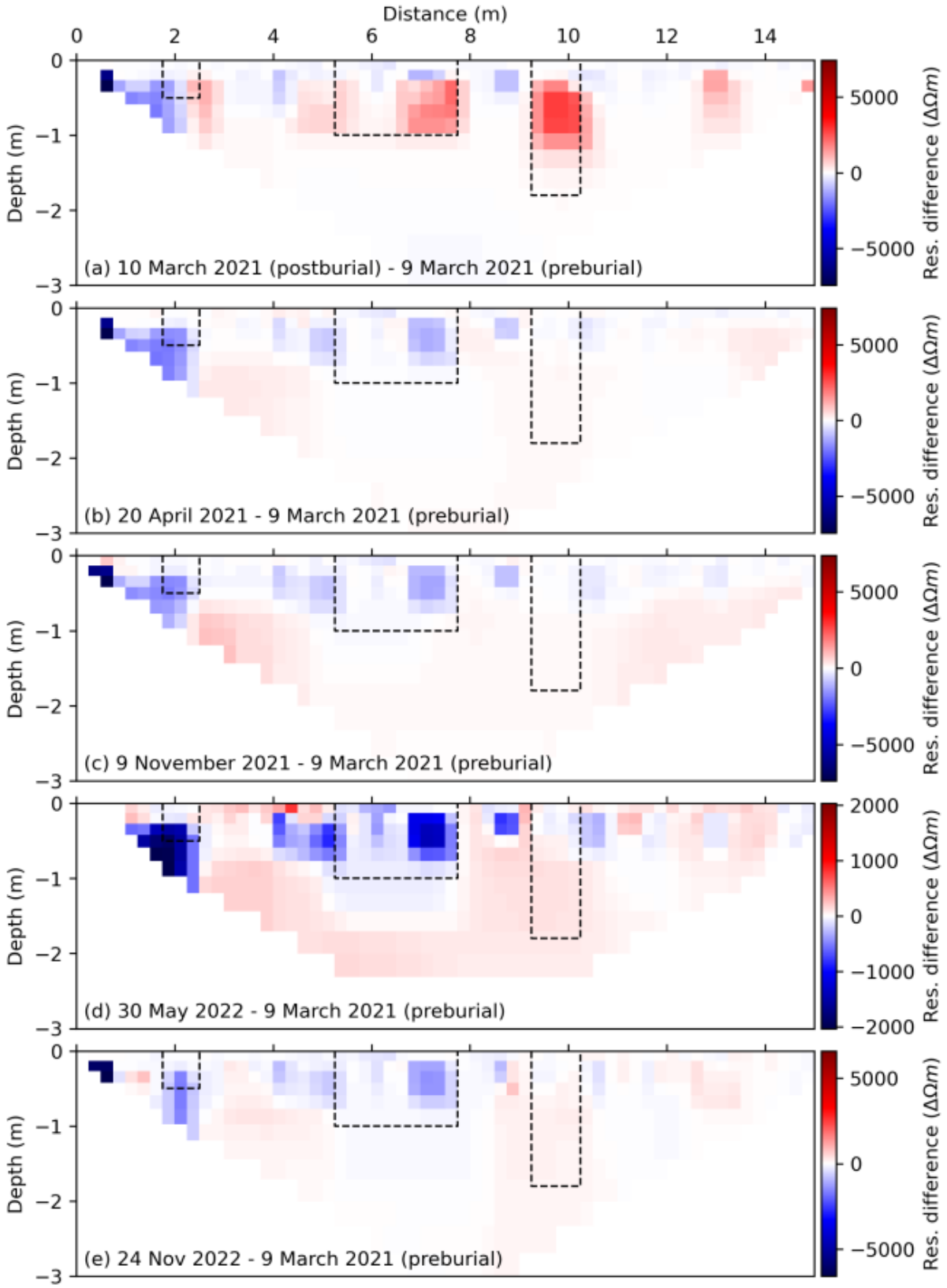


Figure S22. Resistivity difference plots between a) post-burial and pre-burial, b) Apr-21 and pre-burial, c) Nov-21 and pre-burial, d) May-22 and pre-burial, and e) Nov-22 and pre-burial. Red represents an increase and blue represents a decrease in resistivity between two surveys. Wenner data. Difference plots were generated in Python.

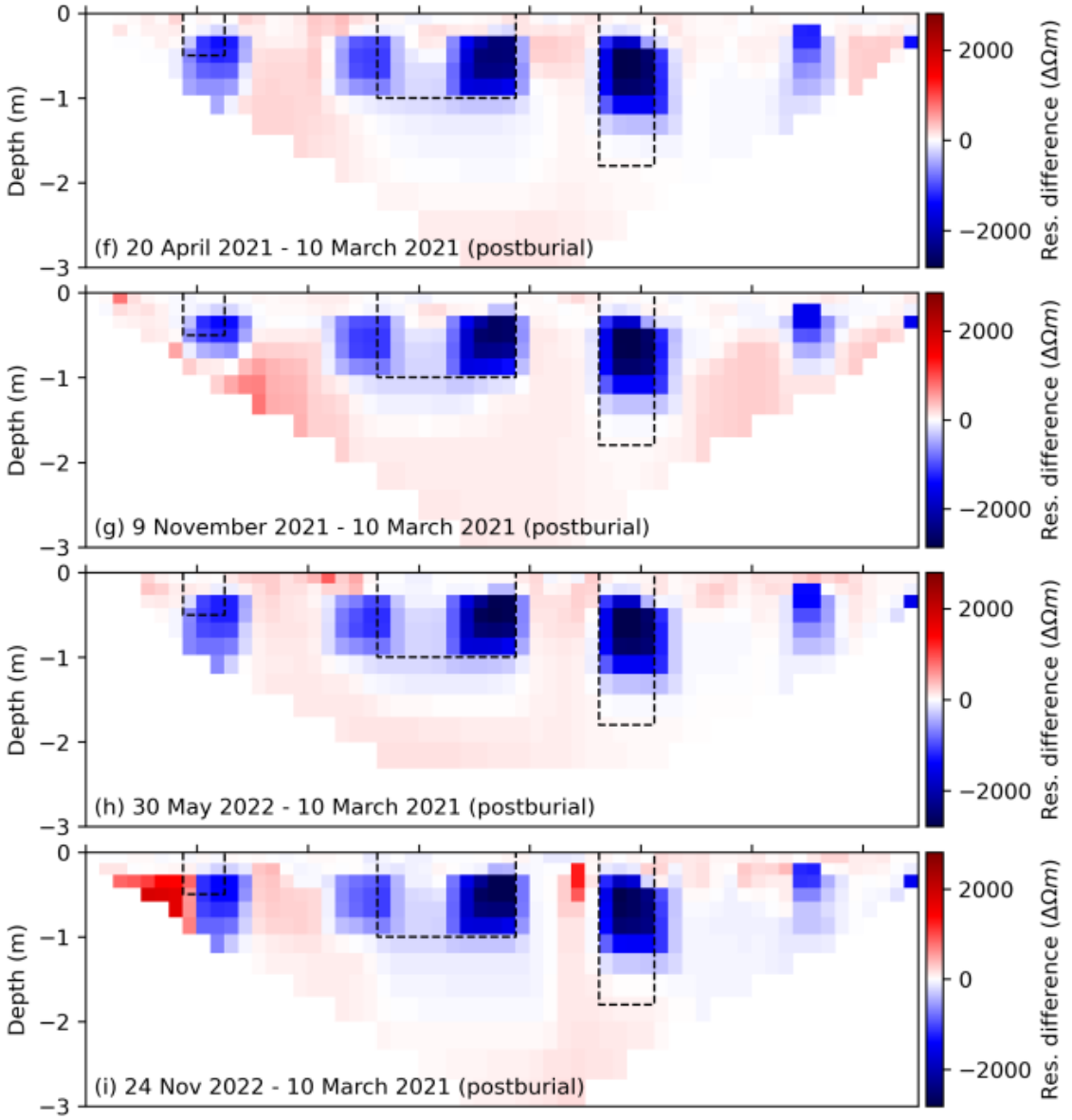


Figure S23. Resistivity difference plots between f) Apr-21 and post-burial, g) Nov-21 and post-burial, h) May-22 and post-burial, and i) Nov-22 and post-burial. Red represents an increase and blue represents a decrease in resistivity between two surveys. Wenner data. Difference plots were generated in Python.

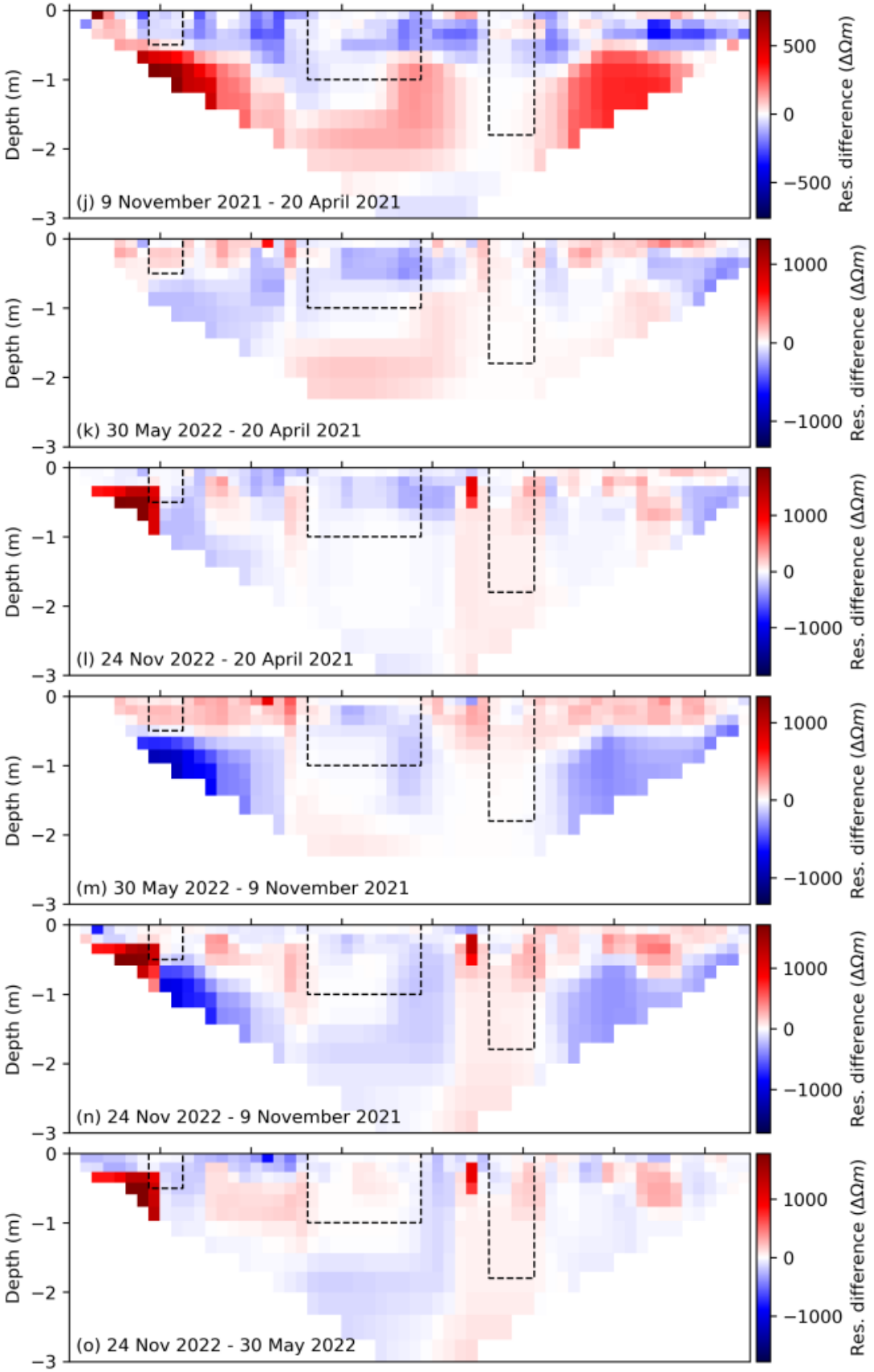


Figure S24. Resistivity difference plots between j) Nov-21 and Apr-21, k) May-22 and Apr-21, l) Nov-22 and Apr-21, m) May-22 and Nov-21, n) Nov-22 and Nov-21, and o) Nov-22 and May-22. Red represents an increase and

blue represents a decrease in resistivity between two surveys. Wenner data. Difference plots were generated in Python.

S3 Soil testing

Ten soil samples in total were taken at various depths from the three graves including: 0.10 m, 0.20 m, and 0.50 m from PS1; 0.15 m, 0.25 m, and 0.60 m from PM1; and 0.10 m, 0.25 m, 0.60 m, and 1.5 m from PS2. Refer to S25 for the soil profile at each of the depths in which soil samples were taken.

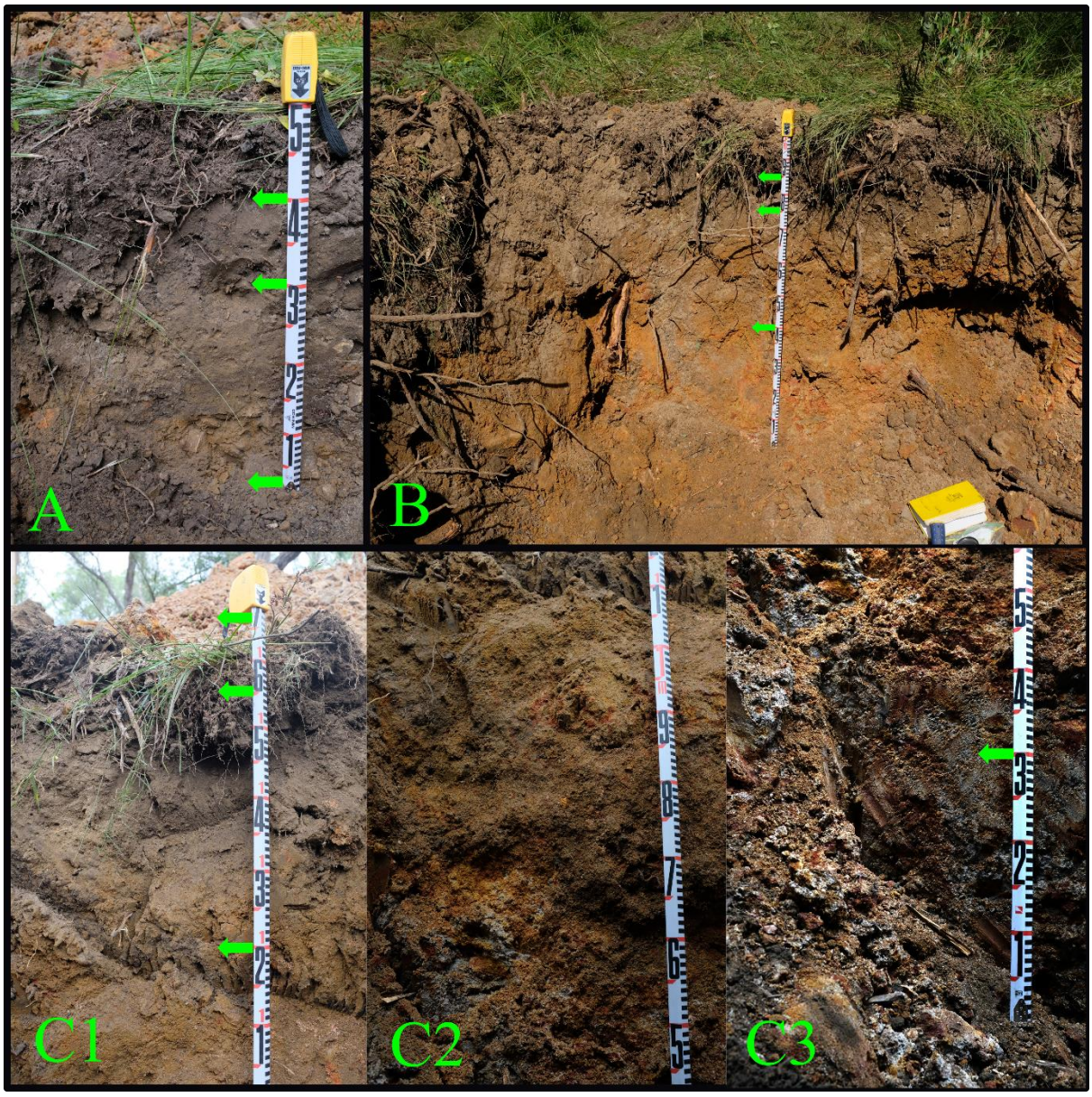


Figure S25. Soil profile at each depth (denoted by a green arrow) that a soil sample was taken from PS1 (A), PM1 (B), and PS2 (C1, C2, and C3).

S3.1 Grain size

The initial weights of the soil samples at each of the grave depths can be found in Table S7. The grain size results, found in Figure S25 and Tables S8-10, show that the soil at the study site consists mainly of fine and very fine-grained sand (59%), with small amounts of clay and silt (average of 16%).

Table S7. Soil sample weights at each grave depth prior to grain size analysis.

PS1		**PM1**		**PS2**	
Grave depth (m)	Total weight (g)	Grave depth (m)	Total weight (g)	Grave depth (m)	Total weight (g)
0.10	126.15	0.15	92.31	0.10	120.30
0.20	105.91	0.25	163.74	0.25	144.55
0.50	138.63	0.60	133.42	0.60	147.10
				1.5	210.54

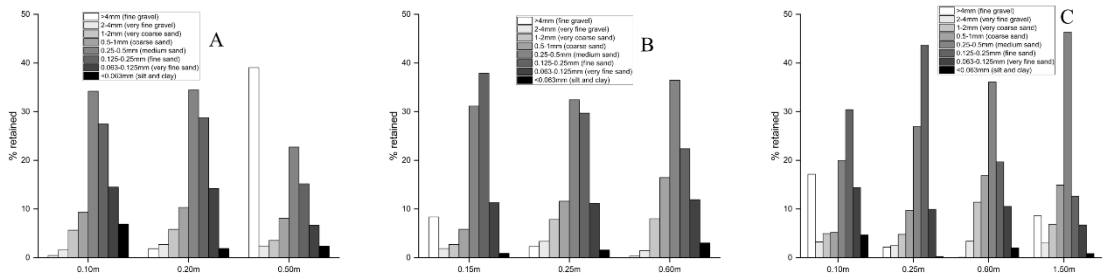


Figure S26. Grain size analysis results for the soil samples taken at the respective grave depths for PS1 (A), PM1 (B), and PS2 (C).

Table S8. Grain size results for PS1.

Krumbein phi scale [Size range (Wentworth class)]	Grave depths					
	0.10m		0.20m		0.50m	
	Weight (g)	% of total	Weight (g)	% of total	Weight (g)	% of total
>4mm (fine gravel)	0.557	0.435	1.955	1.851	54.036	39.056
2-4mm (very fine gravel)	2.013	1.571	2.839	2.688	3.324	2.402
1-2mm (very coarse sand)	7.239	5.650	6.146	5.819	4.885	3.531
0.5-1mm (coarse sand)	11.920	9.304	10.899	10.318	11.231	8.117
0.25-0.5mm (medium sand)	43.808	34.192	36.401	34.462	31.431	22.717
0.125-0.25mm (fine sand)	35.174	27.453	30.373	28.755	21.010	15.185
0.063-0.125mm (very fine sand)	18.576	14.499	14.990	14.191	9.213	6.659
<0.063mm (silt and clay)	8.836	6.896	2.025	1.917	3.226	2.332

Table S9. Grain size analysis for PM1.

Krumbein phi scale [Size range (Wentworth class)]	Grave depths					
	0.15m		0.25m		0.60m	
	Weight (g)	% of total	Weight (g)	% of total	Weight (g)	% of total
>4mm (fine gravel)	7.696	8.360	3.743	2.290	0.432	0.325
2-4mm (very fine gravel)	1.727	1.876	5.470	3.346	1.916	1.440
1-2mm (very coarse sand)	2.487	2.702	12.839	7.854	10.647	8.002
0.5-1mm (coarse sand)	5.365	5.828	18.971	11.606	21.894	16.455
0.25-0.5mm (medium sand)	28.689	31.166	53.033	32.443	48.516	36.464
0.125-0.25mm (fine sand)	34.855	37.864	48.553	29.703	29.782	22.384
0.063-0.125mm (very fine sand)	10.417	11.316	18.264	11.173	15.850	11.913
<0.063mm (silt and clay)	0.816	0.886	2.591	1.585	4.015	3.018

Table S10. Grain size analysis of PS2.

Krumbein phi scale [Size range (Wentworth class)]	Grave depths							
	0.10m		0.25m		0.60m		1.5m	
	Weight (g)	% of total	Weight (g)	% of total	Weight (g)	% of total	Weight (g)	% of total
>4mm (fine gravel)	20.516	17.135	3.278	2.182	0.095	0.065	18.037	8.591
2-4mm (very fine gravel)	3.884	3.244	3.716	2.473	4.930	3.380	6.561	3.125
1-2mm (very coarse sand)	5.915	4.940	7.191	4.786	16.606	11.386	14.399	6.858
0.5-1mm (coarse sand)	6.223	5.197	14.593	9.713	24.620	16.880	31.321	14.917
0.25-0.5mm (medium sand)	23.941	19.995	40.530	26.977	52.648	36.097	97.286	46.335
0.125-0.25mm (fine sand)	36.404	30.405	65.662	43.706	28.716	19.689	26.505	12.624
0.063-0.125mm (very fine sand)	17.238	14.397	14.933	9.940	15.344	10.520	14.073	6.703
<0.063mm (silt and clay)	5.611	4.686	0.334	0.222	2.892	1.983	1.780	0.848

S3.2 Magnetic susceptibility

The magnetic susceptibility results, shown in Figure S26 and Table S11, show that the soil at the research site consisted mainly of diamagnetic materials exhibiting a weak magnetic susceptibility [46].

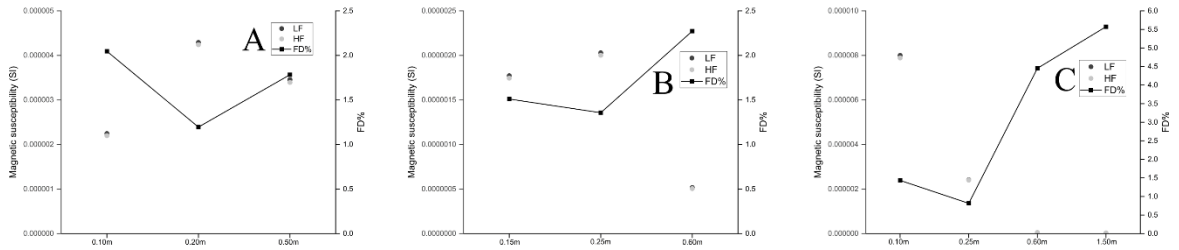


Figure S27. Magnetic susceptibility results. Low frequency (LF), high frequency (HF), and frequency-dependent susceptibility (FD%) for PS1 (A), PM1 (B), and PS2 (C).

Table S11. Magnetic susceptibility analysis results for PS1, PM1, and PS2.

Sample ID (Grave #-depth in cm)	**LF**	**HF**	**FD%**
G1-10	2.25E-06	2.2E-06	2.0
G1-20	4.29E-06	4.24E-06	1.2
G1-50	3.46E-06	3.39E-06	1.8
G2-15	1.77E-06	1.75E-06	1.5
G2-25	2.03E-06	2E-06	1.4
G2-60	5.17E-07	5.06E-07	2.3
G3-10	8E-06	7.89E-06	1.4
G3-25	2.42E-06	2.4E-06	0.8
G3-60	4.84E-08	4.62E-08	4.5
G3-150	2.45E-08	2.31E-08	5.6

S3.3 Soil water content, organic, and carbonate matter fractions

First, each kiln-compatible container was individually weighed, as they each have a slightly different mass. Second, each container was filled with a small sample of soil and weighed again. This was considered each sample's starting weight. Third, the samples were placed in the kiln at 100°C for overnight which removed all the water in each sample. Fourth, the samples were placed in the kiln at 550°C for 4 hours which removed the organic matter. The fifth and final step consisted of the samples being placed in the kiln at 950°C overnight, which removed the carbonate in each sample. It should be noted that in between steps three four, and five, the samples were re-weighed. Once the weights of each sample at each step was compiled, the individual soil, water, organic, and carbonate weights were calculated as a raw value and as a percentage.

The results, shown in Figure S27 and Table S12, show small amounts of water and organic matter, and no carbonate.

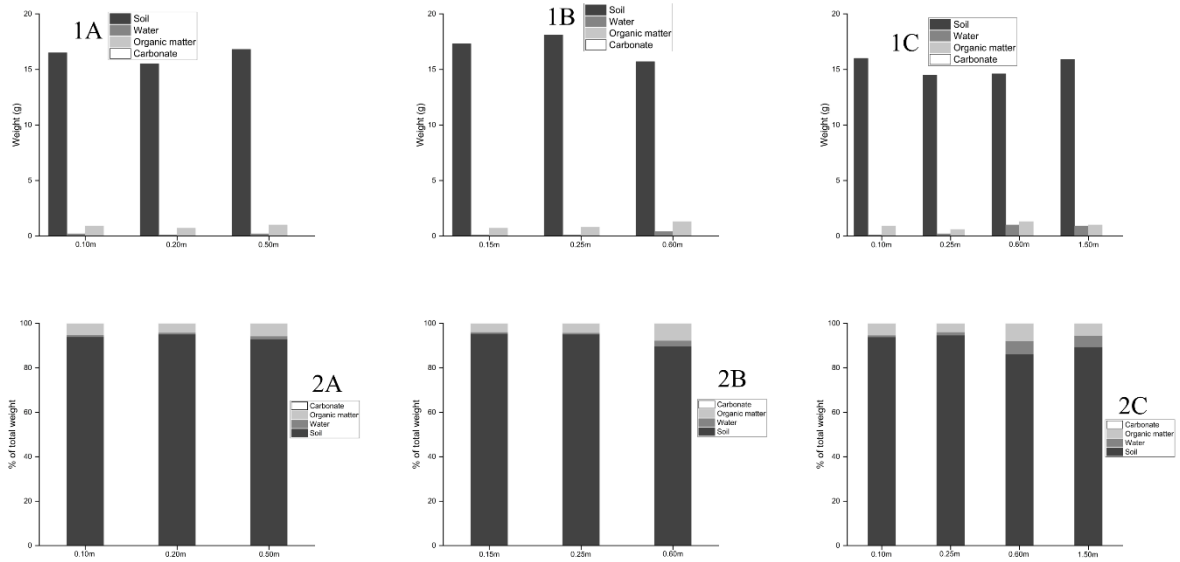


Figure S28. Loss on ignition results. Soil water content, organic, and carbonate matter fractions for PS1 (1A), PM1 (1B), and PS2 (1C), and the percentage of the total weight for each category for PS1 (2A), PM1 (2B), and PS2 (2C).

Table S12. Loss on ignition results demonstrating the soil water content, organic, and carbonate matter fractions of PS1, PM1, and PS2.

Sample ID (Grave #-depth in cm)	**Soil**		**Water**		**Organic matter**		**Carbonate**	
	Weight (g)	% of total	Weight (g)	% of total	Weigh t (g)	% of total	Weight (g)	% of total
G1-10	16.5	94.0	0.2	0.9	0.9	5.1	0.0	0.0
G1-20	15.5	95.1	0.1	0.8	0.7	4.2	0.0	0.0
G1-50	16.8	93.0	0.2	1.3	1.0	5.7	0.0	0.0
G2-15	17.3	95.4	0.1	0.7	0.7	3.9	0.0	0.0
G2-25	18.1	95.1	0.1	0.7	0.8	4.2	0.0	0.0
G2-60	15.7	89.8	0.4	2.5	1.3	7.6	0.0	0.0
G3-10	16.0	93.9	0.1	0.8	0.9	5.3	0.0	0.0
G3-25	14.5	94.7	0.2	1.4	0.6	3.9	0.0	0.0
G3-60	14.6	86.1	1.0	6.0	1.3	7.9	0.0	0.0
G3-150	15.9	89.4	0.9	5.1	1.0	5.4	0.0	0.0

S4 References

46. Dearing, J., *Environmental Magnetic Susceptibility: Using the Bartington MS2 System*. 1999, British Library Cataloguing: UK.